A STUDY OF THE EFFECT OF [illegible] FACTORS UPON THE [illegible] OF AN [illegible]

A REPORT OF WORK CARRIED OUT UNDER TASK ASSIGNMENT NO.1 (modified) OF CONTRACT CST-1224 (DAI-49-186-ORD(P)-100) FOR THE DIAMOND ORDNANCE FUZE LABORATORIES

VIRGINIA MILITARY INSTITUTE
DEPARTMENT OF PHYSICS
LEXINGTON, VIRGINIA

JUNE 30, 1954

ABSTRACT OF REPORT ON EFFECT OF GEOMETRICAL FACTORS UPON THE BEHAVIOUR OF AN UNTUNED CLOCK MECHANISM

Continuing the study of untuned clock mechanisms, the dependence on time delay of the following geometrical factors was determined empirically: (1) the angle at the verge corner, (2) the center to center distance, verge to wheel, (3) the radius of the tooth circle of the wheel, (4) the position of the corner points of the verge with respect to the axis of rotation of the verge. It was found that except in case (1), the empirical relationship[1]

$$T = B \cdot \gamma^{-0.5} I_v^{.612} I_w^{-.112}$$

must be rewritten (the powers of I_v and I_w) to predict times T. The given relationship is correct for the geometrical situation of case (1).

In each of the case (2), (3), and (4) a linear relationship (approximately) is found to hold when values of T are plotted against values of the geometrical factor being varied.

The work ~~abstracted above~~ was actually carried out for a scaled up model of a particular untuned clock mechanism.

1 See a report dated Sept. 1, 1953, entitled "A Study of the Dynamics of an Untuned Clock Mechanism".

R-1

ABSTRACT OF REPORT ON EFFECT OF GEOMETRICAL FACTORS UPON THE BEHAVIOUR OF AN UNTUNED CLOCK MECHANISM

Continuing the study of untuned clock mechanisms, the dependence on time delay of the following geometrical factors was determined empirically: (1) the angle at the verge corner, (2) the center to center distance, verge to wheel, (3) the radius of the tooth circle of the wheel, (4) the position of the corner points of the verge with respect to the axis of rotation of the verge. It was found that except in case (1), the empirical relationship[1]

$$T = B \cdot \gamma^{-0.5} I_V^{.612} I_W^{-.112}$$

must be rewritten (the powers of I_V and I_W) to predict times T. The given relationship is correct for the geometrical situation of case (1).

In each of the case (2), (3), and (4) a linear relationship (approximately) is found to hold when values of T are plotted against values of the geometrical factor being varied.

The work abstracted above was actually carried out for a scaled up model of a particular untuned clock mechanism.

1 See a report dated Sept. 1, 1953, entitled "A Study of the Dynamics of an Untuned Clock Mechanism".

I. INTRODUCTION

This is the second report dealing with the study of an untuned clock mechanism, undertaken under Task Assignment No. 1 (modified), Contract No. CST-1224, now designated as DAI-49-186-ORD(P)-100. The first report, dated September 1, 1953, will be referred to frequently and will be designated simply by the letter R.

R dealt with the dynamical characteristics of the clock mechanism, in particular with the effect of moments of inertia of wheel and verge, and applied torque upon the time delay per revolution. This present report will deal with the effects of various geometrical factors upon this time delay.

II. THE DIFFERENTIAL EQUATIONS OF MOTION

Reference to R, pages 1-19, Appendices A and B, will explain the theoretical methods used to determine the time delay per revolution of a scaled up model of the clock. As described in R, the fundamental equation of motion of the verge-wheel system was solved by making use of a linear approximation to certain non-linear relationships involving the angular positions of wheel and verge. The solutions attained and used were only approximately correct for this reason. However, no results given in R are basically invalid because of this.

We are indebted to Mr. Arthur Hausner, of the Diamond Ordnance Fuze Laboratories, who pointed out to us a method of obtaining solutions for the basic differential equation which does not involve the use of the linear approximations mentioned above. In order to describe this exact method some background material of R will be briefly reviewed.

The clock is an untuned mechanism in which a spring driven toothed wheel engages alternately the leading and trailing pallet faces of a freely oscillating verge. For example, in Fig. 1, a tooth of the wheel is in contact with the leading pallet face. This tooth slides free of the leading pallet face, wheel and verge rotate clockwise and counterclockwise respectively, and then collide at the trailing pallet face. The whole action is then repeated on this trailing face. At each impact energy is lost so that at the end of one cycle the velocity of the wheel is the same as at the beginning of the cycle. Under these circumstances there is a certain average velocity of the wheel, called $\bar{\theta}$.

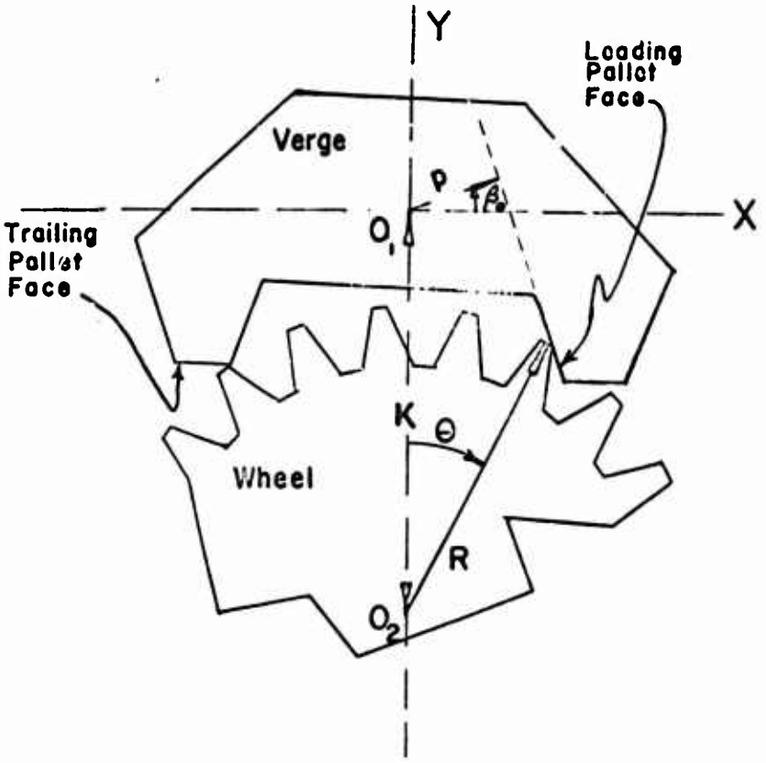

Fig. 1

During the time a tooth is in contact with a pallet face, either leading or trailing we know that

$$\sin(\theta + \beta) = \frac{\rho}{R} - \frac{k}{R}\sin\beta \qquad (1)$$

During this period of contact, each component exerts a torque upon the other, and it is essential that the ratio of the lever arms of these torques be known. This ratio is given by

$$u/v = \frac{R\cos(\theta+\beta)}{\sqrt{(R^2+k^2-p^2)+2kR\cos\theta}} = -\frac{R\cos(\theta+\beta)}{k\cos\beta + R\cos(\beta+\theta)} \qquad (2)$$

Both of these equations are fully discussed in R, II (A) and II (B).

Now if one differentiates (1) he gets (2), or

$$\frac{d\beta}{d\theta} = \frac{u}{v} \qquad (3)$$

This enables us to write

$$-\frac{u}{v} = -\frac{d\beta}{d\theta} = \frac{I_v\ddot{\theta} - \tau}{I_v\ddot{\alpha}} = \frac{d\alpha}{d\theta} \qquad (4)$$

for the fundamental differential equation for leading contact. By separating the variables and integrating

$$\dot{\theta}^2 = \frac{\dot{\theta}_o^2\left[I_w + I_v\left(\frac{d\alpha}{d\theta}\right)_o^2\right] + 2\tau(\theta-\theta_o)}{\left[I_w + I_v\left(\frac{d\alpha}{d\theta}\right)_1^2\right]}$$

Similar considerations lead to an identical solution for trailing contact. This result, which is exact, may be compared with the approximate solution of R, page 16. The change in angle from β to α is fully explained on page 6, R, and represents only a change in axis from which torque angle is measured.

No other equation used in the solution for the motion of the system is changed, although the symbols, γ, γ', K, K', of R will now be replaced by the proper values of $\left(\frac{d\alpha}{d\theta}\right) = u/v$. Of course the fact that we now deal with a different equation of motion than before will necessitate a change in technique of solution. There is therefore included at the end of this report an Appendix A which describes fully the mathematical and arithmetical methods employed. The values of $\dot{\theta}$ computed and used in this report were computed by the exact method unless otherwise noted. No numerical solutions are included in this report; results only are given.

III. SOME THEORETICAL CONSIDERATIONS

In discussing the effect of geometry upon the behaviour of the motion of the system there are certain broad statements which might be made. Intuitively one would expect that any geometry which results in a cycle of a relatively long period of free motion would be characterized by a large value of $\bar{\theta}$. Similarly one expects that if the ratio u/v is relatively large then the value of $\bar{\theta}$ will be relatively small and vice versa. From the results of the empirical work described in the body of this report the above statements will be shown to be true. It is also possible that if one makes certain simplifying assumptions these results may be predicted theoretically.

(A) Cycle of No Free Motion

We assume here that a geometry exists such that as the tooth in leading contact comes to last contact leading and slips free, that immediately the trailing tooth collides with the trailing pallet face, so that there is no free motion at all. We shall further assume that the ratio of lever arms $u/v = d\alpha/d\theta = \gamma$, is a constant. The numerical value of γ is the same for both leading and trailing, but is negative or positive, respectively. The question as to the possibility of constructing a verge for which γ = constant is discussed in Appendix B. We assume finally that the angular distance $\Delta\theta$ through which the wheel moves on leading contact is equal to the $\Delta\theta$ through which the wheel moves on trailing contact. Actual computation of many cycles indicates that this last assumption is very nearly fulfilled in all except the most extreme cases. Referring now and throughout the remainder of this section to the material of Appendix A, one proceeds as follows:

$$\dot{\theta}_1^2 = \dot{\theta}_0^2 + \frac{2\gamma\Delta\theta}{I_w + \gamma^2 . I_v} \qquad (1)$$

since $\left(\frac{d\alpha}{d\theta}\right)_0 = \left(\frac{d\alpha}{d\theta}\right)_1 = \gamma$

and $\theta_1 - \theta_0 = \Delta\theta$. It is to be noted that $\Delta\theta$ is one half the size of the angular tooth spacing (.2856 radians in this clock).

Since there is no free motion a collision takes place immediately at the angle of last contact leading, θ_1 above. We have then

$$\dot{\theta}_3 = \frac{I_w\dot{\theta}_2 + \left(\frac{d\alpha}{d\theta}\right)_3 I_v \left(\frac{d\alpha}{d\theta}\right)_1 \cdot \dot{\theta}_1}{I_w + I_v \left(\frac{d\alpha}{d\theta}\right)_3^2} \qquad (2)$$

which becomes $\dot{\theta}_3 = \frac{I_w\dot{\theta}_1 - \gamma^2 I_v \dot{\theta}_1}{I_w + \gamma^2 I_v} = \frac{I_w - \gamma^2 . I_v}{I_w + \gamma^2 . I_v} \cdot \dot{\theta}_1$

since $\dot{\theta}_2 = \dot{\theta}_1$ and $\left(\frac{d\alpha}{d\theta}\right)_3 = -\left(\frac{d\alpha}{d\theta}\right)_1$

Now we are on trailing contact and can write

$$\dot{\theta}_4^2 = \dot{\theta}_3^2 + \frac{2\tau\Delta\theta}{I_w + \gamma^2 . I_v} \qquad (3)$$

as we have done above, and finally

$$\dot{\theta}_6 = \frac{I_w - \gamma^2 . I_v}{I_w + \gamma^2 . I_v} \cdot \dot{\theta}_4 = \dot{\theta}_o \quad \text{(at equilibrium)} \qquad (4)$$

A simultaneous solution of equations (1) to (4) above gives

$$\dot{\theta}_1^2 = \dot{\theta}_4^2 = \frac{\tau\Delta\theta\,(I_w + I_v\gamma^2)}{2\,I_w\,I_v\,\gamma^2} \qquad (5)$$

$$\dot{\theta}_o^2 = \dot{\theta}_3^2 = \dot{\theta}_6^2 = \frac{\tau\Delta\theta\,(I_w - I_v\gamma^2)^2}{2\,I_w\,I_v\,\gamma^2\,(I_w + I_v\gamma^2)} \qquad (6)$$

and we have the final and initial velocities of each half of the cycle expressed in terms of the geometrical and dynamic constants of the system. Note that it is possible that $\dot{\theta}_o$ should be negative, in which case the wheel backs up and then goes forward. This possibility is <u>not</u> considered.

Now the two halves of the cycle are of course identical so the average velocity over one half is the average over the whole cycle. To find this we write

$$\dot{\theta}_1^2 = \dot{\theta}_o^2 + \frac{2\tau(\theta - \theta_o)}{I_w + I_v\gamma^2} = a\theta + b$$

where

$$a = \frac{2\tau}{I_w + I_v\gamma^2} \qquad b = \dot{\theta}_o^2 - \frac{2\tau\theta_o}{I_w + I_v\gamma^2}$$

now $T = \int_{\theta_o}^{\theta} \frac{d\theta}{\dot{\theta}_1}$ is time for half cycle.

Integrating gives

$$T = \frac{2}{a}\,(\dot{\theta}_1 - \dot{\theta}_o)$$

so that $\bar{\dot{\theta}} = \frac{\Delta\theta}{T} = \frac{a\,\Delta\theta}{2(\dot{\theta}_1 - \dot{\theta}_o)}$

Substituting equations (5) and (6)

$$\dot{\theta} = \sqrt{\frac{I_w \tau \Delta\theta}{2 I_v \gamma^2 (I_w + I_v \gamma^2)}} \qquad (7)$$

as average or terminal velocity of this cycle.

(B) Cycle of No Contact Motion

Using the same basic assumption as above we now require a geometry such that there is no sliding contact of a tooth on a pallet face. The collisions, both leading and trailing, take place at the positions of last contact. Hence there is contact between tooth and verge only at the instant of collision.

It is wiser here to adopt slightly different equations of motion than those of Appendix A for the free motion, as follows. We write

$$\dot{\theta}_1^2 = \dot{\theta}_o^2 + \frac{2\tau\Delta\theta}{I_w} \qquad (1)$$

where $\dot{\theta}_o$ = velocity of verge immediately after leading collision and $\dot{\theta}_1$ is the velocity at any instant to and including the instant of trailing contact. $\Delta\theta$ is the angular duration of the free motion and is one half of the total angular duration of the cycle.

After the trailing collision

$$\dot{\theta}_2 = \frac{I_w \dot{\theta}_1 - \gamma^2 I_v \dot{\theta}_o}{I_w + I_v \gamma^2} \qquad (2)$$

During the free motion to leading collision

$$\dot{\theta}_3^2 = \dot{\theta}_2^2 + \frac{2\tau\Delta\theta}{I_w} \qquad (3)$$

and just after leading collision

$$\dot{\theta}_4 = \dot{\theta}_o = \frac{I_w \dot{\theta}_3 - \gamma^2 I_v \dot{\theta}_2}{I_w + \gamma^2 I_v} \qquad (4)$$

These equations most simply describe the motion.

To find the time required for one half cycle we integrate

$$T = \int_{\theta_o}^{\theta_f} \frac{d\theta}{\dot{\theta}_1} .$$

which give $T = \frac{2}{a}(\dot{\theta}_1 - \dot{\theta}_0)$

$$\text{or } \bar{\dot{\theta}} = \frac{\Delta\theta}{T} = \sqrt{\frac{\tau \cdot \Delta\theta \cdot (I_w + I_v \gamma^2)}{2 I_w I_v \gamma^2}} \qquad (5)$$

This follows from (1), (2), (3), (4) and the expression for T.

(C) Comparision of Results

We now compare the results shown above.

All Contact Motion	All Free Motion
$\bar{\dot{\theta}} = \sqrt{\frac{\tau \cdot \Delta\theta}{2 I_w I_v \gamma^2} \cdot \frac{I_w^2}{I_w + I_v \gamma^2}}$	$\bar{\dot{\theta}} = \sqrt{\frac{\tau \Delta\theta}{2 I_w I_v \gamma^2} \cdot (I_w + I_v \gamma^2)}$

A cursory inspection of these equations allows us to conclude that (1) the cycle of free motion has a larger average velocity than that of contact motion, (2) as $\gamma = u/v$ increases, the average velocity associated with any cycle will decrease. These results agree with the predictions made at the beginning of the cycle.

The work of this paragraph was done by Mr. Arthur Hausner of Diamond Ordnance Fuze Laboratories and is included in this report for convenience.

IV. GEOMETRICAL FACTORS EFFECTING THE MOTION

Reference to Appendix A of this report will allow one to examine all equations used in the solution for the motion of the system. A very brief inspection is sufficient to impress upon one the importance of the curves α vs θ, and u/v vs θ in determining the motion. Any factor influencing the shape of the curves will inevitably influence the average velocity $\dot{\theta}$. Referring back to Section II, one is able to see that these curves will depend upon the terms β_o, k, R, p, each of which is a definite geometrical factor of the system. The diagram of Fig. 1 shows these quantities where β_o is that particular value of β for which the verge is in equilibrium.

One would of course, consider the possibility of expressing $u/v = d\alpha/d\theta$ in terms of these quantities (and β and θ) and by substitution into the equations of motion be able to make theoretical predictions about the effect of any one factor upon $\dot{\theta}$. Unfortunately the family of equations (Appendix A) that one must use in order to plot a curve $\dot{\theta}$ vs θ is of such a nature that even though every equation in the list be expressed in terms of β_o, k, R, and p, it is still not possible to arrive at any analytical expression for $\dot{\theta}$. If this were possible we could of course have proceeded in just this way to establish the functional dependence of $\dot{\theta}$ on I_v, for example. Basically, the motion of this system is treated as discontinuous at each collision, and this fact is in large part responsible for the trouble discussed above.

After several abortive attempts to work out some theoretical method of handling this problem it became evident that we were faced with the necessity of proceeding empirically; i.e. computing $\dot{\theta}$ for each of the various geometrical possibilities and attempting to derive some information from these results. This is a long and tedious procedure, and a repetition again and again of a fixed method of solution. Only results of such solutions are given in this report.

One of the factors appearing in the list above is p, which is given by the equation

$$p = x_o \cos\beta_o + y_o \sin\beta_o$$

In this equation $(x_o y_o)$ represent the coordinates of the leading verge-point, when the verge is in equilibrium. These coordinates are referred to a set of axes marked x and y in Fig. 1, having origin O_1. It was considered wise to think of the geometrical factors, then, as

$$\beta_o,\ k,\ R,\ (x_o y_o)$$

In our computations only one factor was varied at a time, all others being held constant. The factor to be varied was taken for several specific values over its allowable range, and for each such value $\dot{\theta}$ was computed for two or three values of I_v. From the results reported in R we believe that the functional dependence of $\dot{\theta}$ on τ will not be changed by any reasonable change in geometry. The functional dependence of $\dot{\theta}$ on I_v is determined from a study of the dependence of $\dot{\theta}$ on I_v. For these reasons values of $\dot{\theta}$ were computed (for the various geometries) only with different I_v.

Finally we based all our computations upon the scaled up model. The value of torque always used is 2.71×10^6 dyne-cm. The moment of inertia of the wheel is 2079 gm-cm^2. Since the geometrical curves represent only angles, or ratios, the geometrical dimensions can be expressed either in terms of the model or of the actual clock.

(A) Limits of β_o

β_o is the angle made by p with the positive x axis when the verge is at leading equilibrium, as shown in Fig. 3. It is also, a face angle and is a measure of the slope of the leading pallet face. Although we shall talk about angles β_o in terms of the leading verge corner, one could just as easily adopt the discussion to the case of β_o measured at the trailing corner.

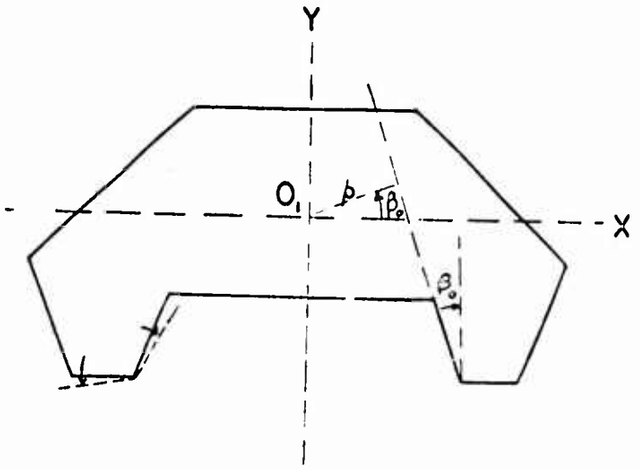

FIG. 3

In varying β_o we increased or decreased the angles of the faces of the verge by equal amounts at each corner. The dotted lines at the trailing corner of the verge in Fig. 3, shows how this is done. To find limits here, means to find how sharp or how obtuse we can make these corners and still have the system run normally.

Remember that no other dimensions (including the positions of corner points) are changed at all. Reference to Figure 4 will make the geometrical procedure clear. We imagine that following last contact leading the wheel remains in position and the verge turns to meet it, either tooth 1 against face 1, or tooth 2 against face 2. If tooth 2 collides with face 2 before tooth 1 collides with face 1 we no longer have "normal" motion, and a limit will be placed on both maximum and minimum values of β_o . It actually turns out that at $\beta_o = 29.5^\circ$ we have an upper limit and at $\beta_o = 7.5^\circ$ there is a lower limit, where $\beta_o = 17.5^\circ$ is the value for the "normal" verge, i.e. the actual verge used in the clock. This information about limits is found by determining the distance of tooth 2 from face 2 when face 1 strikes tooth 1 for various

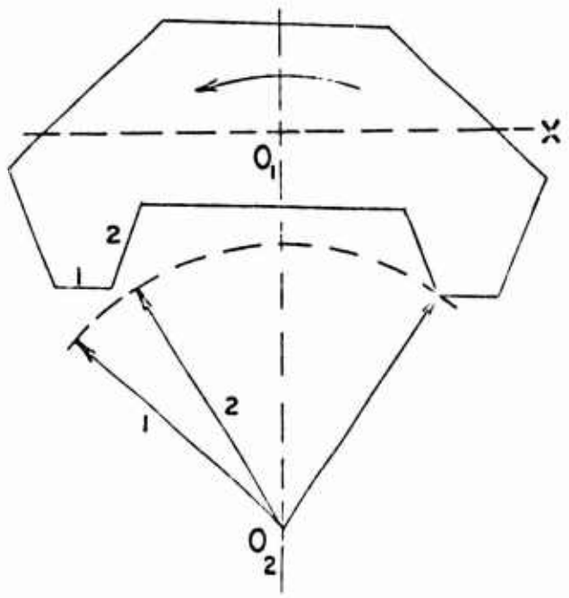

FIG. 4

values of β_o. It is found that as β_o increases from 17.5° the teeth 1 and 2 come nearer to a condition in which both will strike the verge simultaneously. When β_o = 29.5° they do strike simultaneously (or nearly so) and if β_o is made any larger then tooth 2 collides first, which is not "normal" motion. In a similar way (at leading collision) the lower limit is found. The computations are simple but laborious and are not shown.

We should note that our assumption that the wheel stays at rest after last contact and waits for the verge to come around and strike it is of course untrue. Actually the wheel turns into the verge, and this of course puts tooth 1 into a more favorable position to collide first. There is no way of accounting for this geometrically, so our upper and lower limits are probably a little too near the "normal" value. We use them regardless.

(B) Limits of k

The term k represents the distance between centers of the verge and wheel. Certainly as k is made larger the verge interferes less with the rotation of the wheel and if k is too large the wheel is able to turn freely without being slowed down by the verge. The upper limit on k will be that at which the two corners of the verge are on the tooth circle. Simple geometry gives k = .2269 for this value.

Now as k decreases, the verge moves in toward the wheel and will eventually cause it to jam if it is too close. This jamming occurs when tooth 1 (see Fig. 4) is in contact with face 1 at the instant of last contact leading. If one finds the distance from the tip of tooth 1 to the face 1 of the verge for conditions of last contact loading at various values of k, then it turns out that a k = .2172, tooth tip 1 is just touching face 1, Any k smaller than this will result in jamming.

(C) Limits on R

R is the radius of tooth tip circle for the wheel. As R becomes smaller the verge has less and less influence on the wheel and if R is so small that the points of the verge lie outside the tooth circle then the wheel can run freely. The lower limit on R is therefore that value of R such that the leading and trailing verge corners lie on the tooth circle simultaneously. This value is R = 0.1640.

The upper limit on R is found precisely as is the lower limit of k, described above. The computation is long and tedious but does give the result, which is R = .1740.

(D) Limits on $(x_o y_o)$

The coordinates $(x_o y_o)$ locate the position of the verge point with reference to O_1 when verge is in equilibrium position. This is the most difficult case as far as determining limits is concerned. It appeared wise to discuss first the limits on ρ where $\rho^2 = x_o^2 + y_o^2$

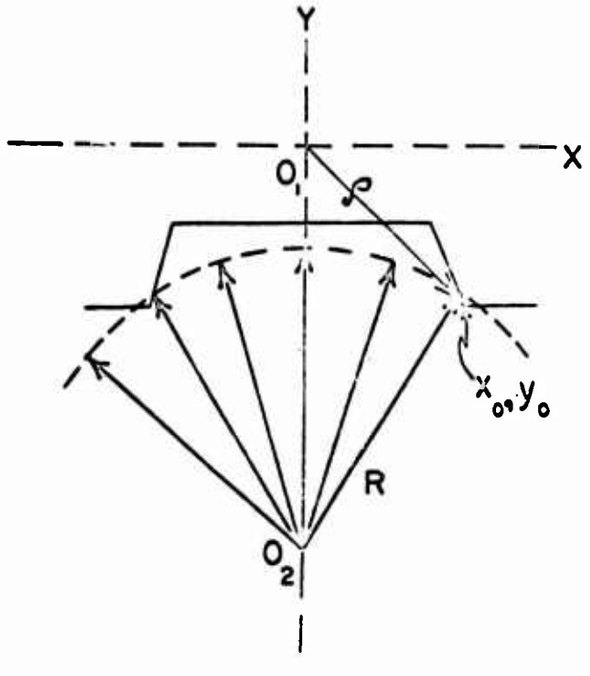

FIG. 5

Of course all tooth points lie on the dotted circle, Fig. 5, and if ρ is such that the two corner points of the verge lie on this circle at equilibrium position then this will be a limit on ρ. Clearly there is a range of values of ρ for which this geometrical condition is met. If the behaviour of the system is to be normal, we can begin by agreeing that the two verge corners must subtend an angle on the wheel no greater than five tooth spaces, nor less than four. Using this idea, we can find that the limits on ρ are .1217 and .1456. The coordinates $(x_o y_o)$ in each case are (.091, -.081) and (.110, -.096) and these points are lying on the tooth circle. No points $(x_o y_o)$ (for any given value of ρ within the permitted range) may be chosen lying outside the tooth circle, but points lying inside are permitted. Curve 1, Fig. 6, is a plot of all the possible points lying on the tooth circle, with the values of ρ written in at intervals.

The next problem will be to find, for each possible value of ρ within the above range, the limits on the angle $2\gamma_o$, shown in Fig. 7. This of course will put limits on the points $(x_o y_o)$ associated with each value of ρ. In this way we may map out the total region within which the corner point of the verge $(x_o y_o)$ may lie.

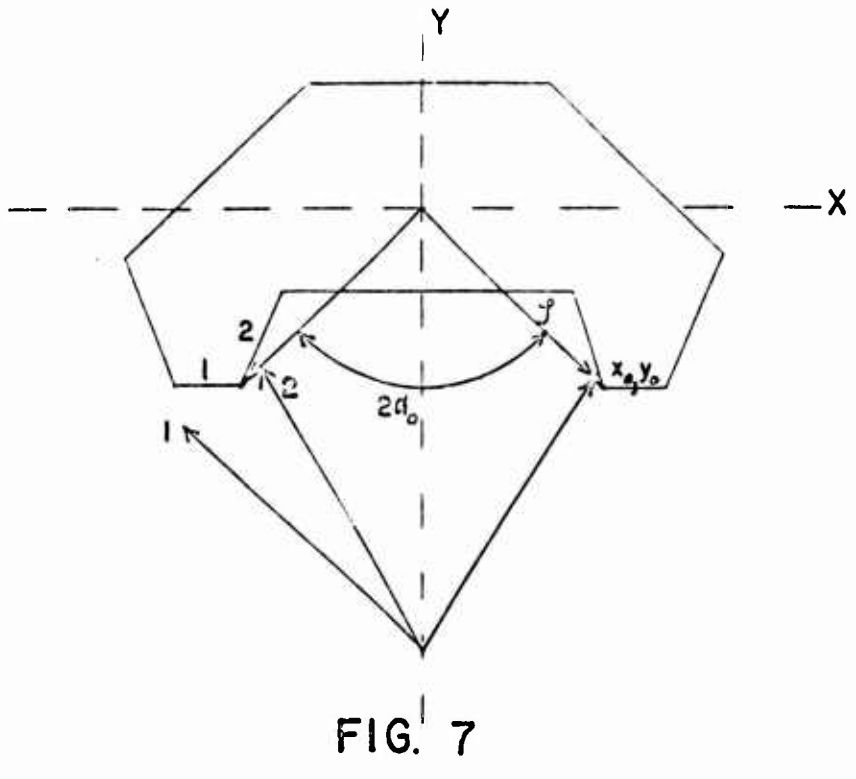

FIG. 7

The upper limit of $2\gamma_o$ has already been established by the above described work, so that we need to discuss only the lower limit. There are two ways, physically, in which this lower limit might occur. (1) $2\gamma_o$ so small that at last contact leading, tooth number 2 is already in contact with face 2 of the trailing verge. (2) $2\gamma_o$ is so small that at last contact leading tooth number 1 is already in contact with face 1 of the trailing verge.

Now if case (1) occurs we must investigate further, because "normal" motion does not allow the collision to take place in this manner. Hence in such regions that case (1) occurs we must further limit $2\gamma_o$ by finding values of $2\gamma_o$ for which tooth 1 collides with face 1 at the same time that tooth 2 collides with face 2. The computations are very long, but the results, shown in Fig. 6 are easy to interpret. These results, originally expressed in terms of γ_o are plotted in terms of $(x_o y_o)$, as can easily be done. (Refer to Fig. 7).

Curve 1 has already been discussed. Curve 2 gives the limiting values of the points $(x_o y_o)$ as determined by the fact that tooth 2 is in contact with face 2 at last contact leading. To have the verge corner at a point to the left of this curve would result in jamming the system. Curve 3 gives limiting values of $(x_o y_o)$ determined by the fact that at last contact leading tooth 1 is in contact with face 1. Again, if the verge corner should lie below this curve, the system would jam. Remembering that the "normal" motion does not allow tooth 2 to slide on face 2, we next refer to Curve 4. Along this curve, both teeth 1 and 2 are simultaneously in contact with faces 1 and 2 and at last contact leading at any point to the left and above this line tooth 2 strikes the verge first, to the right and below it is tooth 1 which limits the values of $(x_o y_o)$. The region lightly crosshatched, bounded by curves 1, 2, and 3 is not allowed. Finally, then, all points $(x_o y_o)$ lying in the region bounded by Curves 1, 3 and 4 are geometrically allowable.

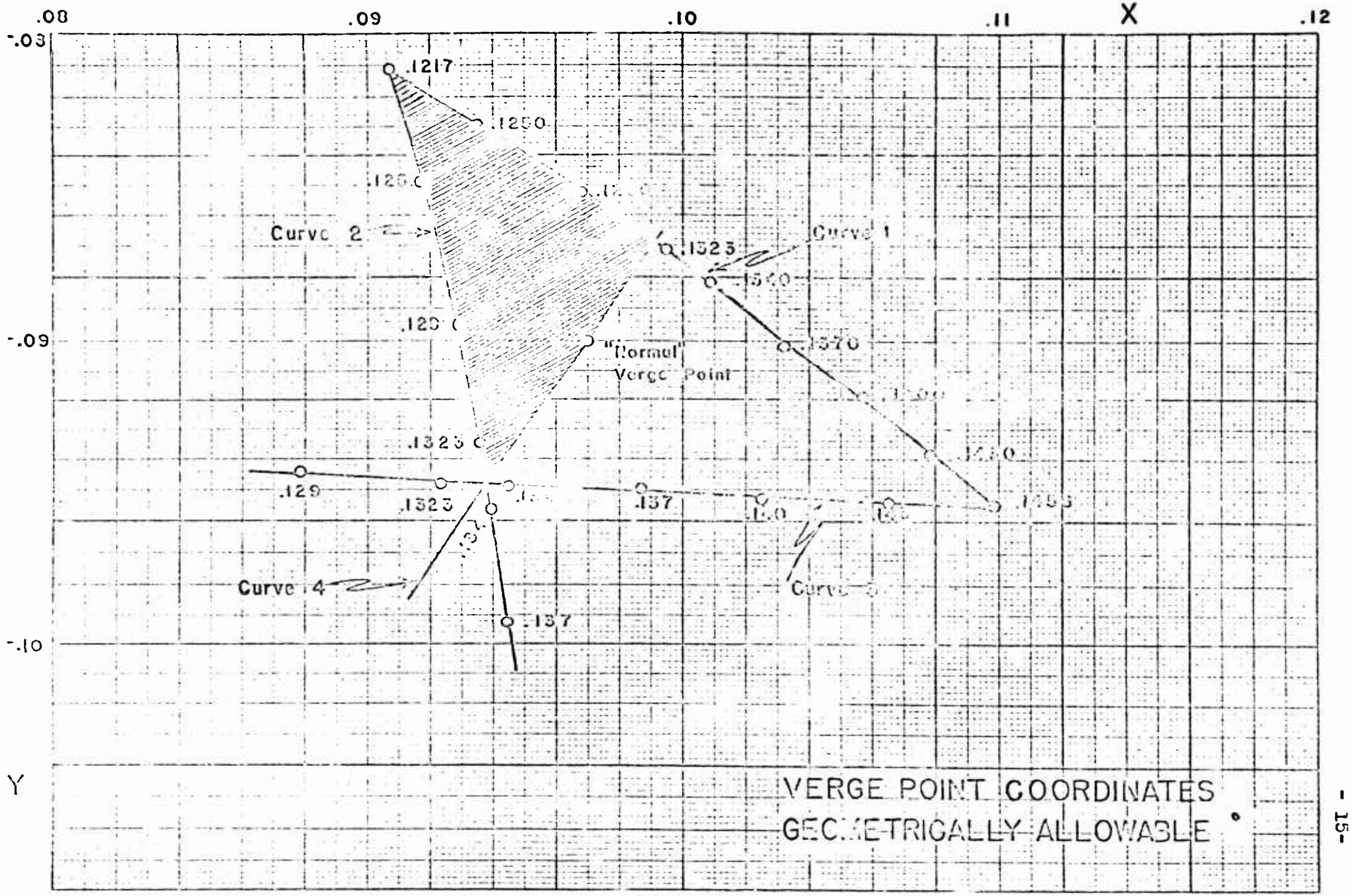
.08
.09
.10
.11
X
.12
-.08
-.09
-.10
Y
.1217
.1250
Curve 2
.1523
Curve 1
.1540
"Normal"
Verge Point
.1570
.129
.1323
.137
Curve 4
.137
VERGE POINT COORDINATES
GEOMETRICALLY ALLOWABLE

FIG. 6

Curiously enough the "normal" verge point lies just on the left boundary of this region. For future reference we record below the values of $(x_o y_o)$ used in computing velocities.

ρ = .1323		ρ = .1340	
x_o = .096	y_o = -.091	x_o = .096	y_o = -.089
x_o = .097	y_o = -.090	x_o = .098	y_o = -.091
x_o = .098	y_o = -.089	x_o = .100	y_o = -.094
ρ = .1370		ρ = .1400	
x_o = .1000	y_o = -.0936	x_o = .1040	y_o = -.0936
x_o = .1020	y_o = -.0915	x_o = .1050	y_o = -.0937

ρ = .1430
x_o = .1074
y_o = -.0944

(E) The "Normal" Verge

For reference, the values of the geometrical constants are

R = .16775 $\quad$ β_o = 17.5° $\quad$ x_o = .096
k = -.2222 $\quad$ y_o = -.090

VI. THE VARIATION OF $\bar{\dot{\theta}}$ WITH β_o

Work had been done on this variation before R was written, and is mentioned in Section VI (G). All calculations for variation in β_o were carried out by the old method, using approximate solutions to the differential equations.

β_o was varied in steps of 2° from the lower limit of 7.5° to the upper limit of 27.5°. The value of $\bar{\dot{\theta}}$ was computed for six different verge moments of [illegible] at each value of β_o. The results of all these calculations are [illegible] on the graph of Fig. 8. Several of these points are quite probably numerically incorrect, as shown by the fact that they lie off the curves, but the burden of calculation was so great that they were not recomputed.

The most striking feature of these curves is the apparent flattening or step occuring in the neighborhood of the normal value, $\beta_o = 17.5°$, a flattening which is more pronounced at the larger verge moments. A later reference to certain experimental results will also give some slight evidence for this same thing. The magnitude of this step in the theoretical curves may be exaggerated by the inexact method of solution used to obtain these values. Recalling that the whole solution depends upon our ability to make accurate linear approximations to these curves, and since all calculation for one value of β_o were based on the same curves, it is readily seen that all values of $\bar{\dot{\theta}}$ for a given β_o might be too large or too small. In any case no direct use of this flattening is made.

The final result of R was an empirical equation for the "normal" verge and wheel

$$\bar{\dot{\theta}} = A \tau^{.45} I_V^{-.612} I_W^{.112} \qquad (1)$$

where we would expect A to be a function of the geometrical dimensions, i.e.

$$A = A(\beta_o, k, R, x_o, y_o)$$

Of course we must note the possibility that the functional relationship expressing $\bar{\dot{\theta}}$ may be different for different geometries since this equation was obtained empirically for one particular geometry only. In particular, one would expect that the exponent of I_V might change.

We begin to analyze our data by substituting into equation (1) above the values for τ, I_V, I_W and for $\bar{\dot{\theta}}$ and computing the resulting values of A. The results are given in the table.

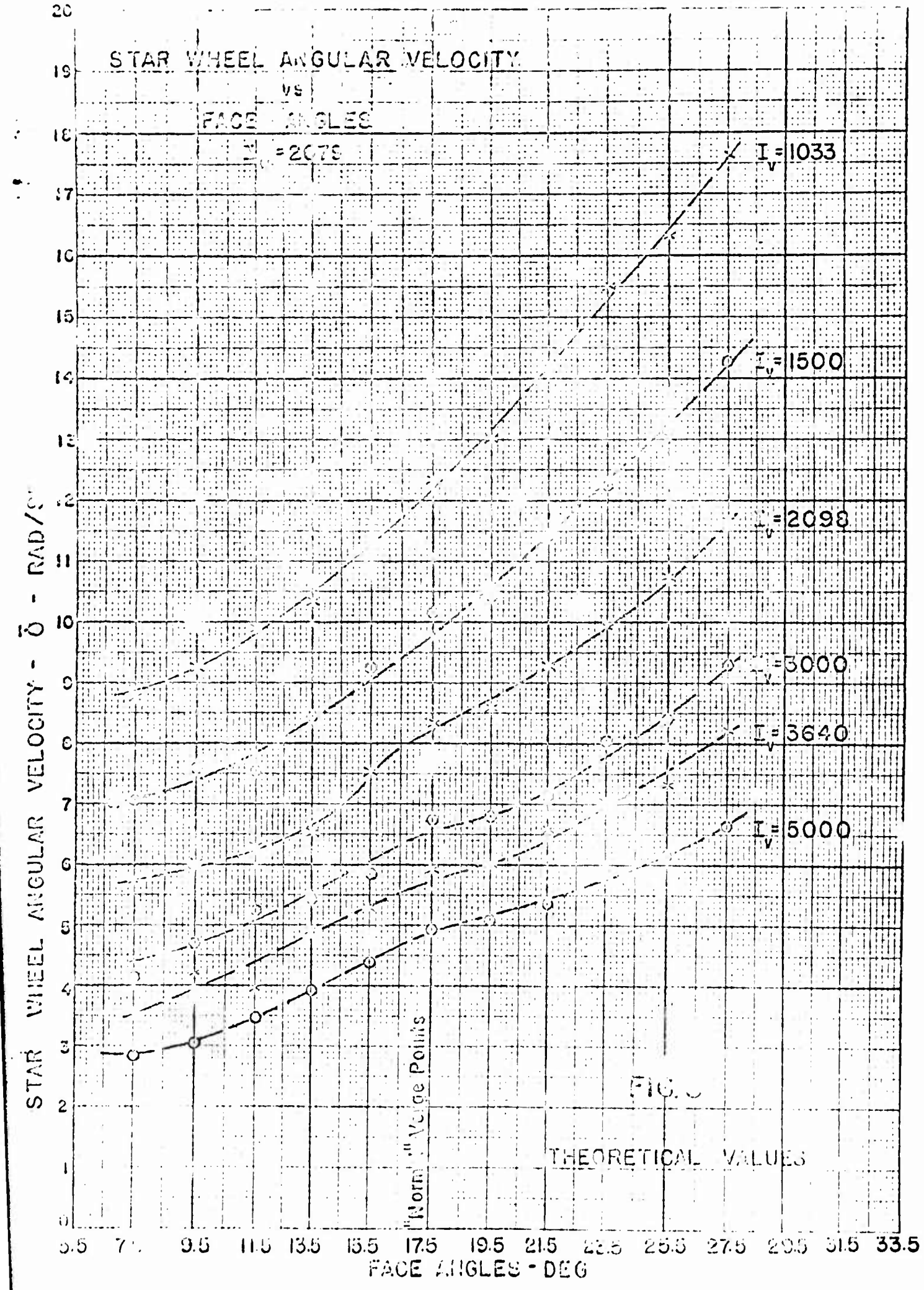
STAR WHEEL ANGULAR VELOCITY
vs
FACE ANGLES
I = 2078
I_v = 1033
I_v = 1500
I_v = 2098
I_v = 3000
I_v = 3640
I_v = 5000
THEORETICAL VALUES
Normal Wedge Points
STAR WHEEL ANGULAR VELOCITY - Ō - RAD/S
FACE ANGLES - DEG
20
19
18
17
16
15
14
13
12
11
10
9
8
7
6
5
4
3
2
1
0
5.5
7.5
9.5
11.5
13.5
15.5
17.5
19.5
21.5
23.5
25.5
27.5
29.5
31.5
33.5

FIG.

I_v	7.5°	9.5°	11.5°	13.5°	15.5°
1033	.158	.166	.178	.186	.210
1500	.160	.171	.172	.191	.210
2098	.159	.168	.175	.181	.208
3000	.145	.163	.182	.189	.204
3640	.139	.164	.153	.189	.205
5000	.137	.144	.165	.187	.209
	.150±.009	.163±.006	.174±.004	.187±.003	.208±.002

I_v	19.5°	21.5°	23.5°	25.5°	27.5°
1033	.234	.255	.279	.294	.317
1500	.236	.258	.277	.299	.323
2098	.237	.258	.275	.298	.323
3000	.236	.247	.279	.292	.322
3640	.229	.256	.274	.285	.319
5000	.242	.251	.279	.289	.314
	.236±.003	.254±.004	.277±.002	.295±.004	.320±.003

Except at the small values of β_o, the mean deviation of the values of A is in the neighborhood of 2%, which would indicate that the functional dependence of C on I_v is not essentially different for different verge angles.

To corroborate this theoretical result, experimental data was obtained with verges whose angles were 9.5°, 13.5°, 15.5°, 19.5°, 21.5° and 25.5°. The results are shown on Fig. 9. It can be seen that the values obtained for the lightest verge are very erratic. In these curves there is only a very slight indication of the flattenning effect noted in the theoretical curves. If one computes the values of A from these experimental data, the following are the results:

I_v	9.5°	13.5°	15.5°	17.5°
1028	.163	.170	.180	.195
1578	.156	.174	.186	.194
2078	.153	.180	.196	.203
2578	.153	.174	.195	.205
3028	.149	.171	.189	.201
	.155±.004	.174±.003	.189±.005	.199±.005

I_v	19.5°	21.5°	25.5°
1028	.188	.201	.209
1578	.200	.213	.234
2078	.212	.226	.237
2578	.216	.220	.234
3028	.214	.220	.239
	.206±.010	.216±.007	.231±.008

Here again, except for the experimental scattering, the values of A are uniform indicating, as before, that we have the correct functional relationship as far as I_v is concerned.

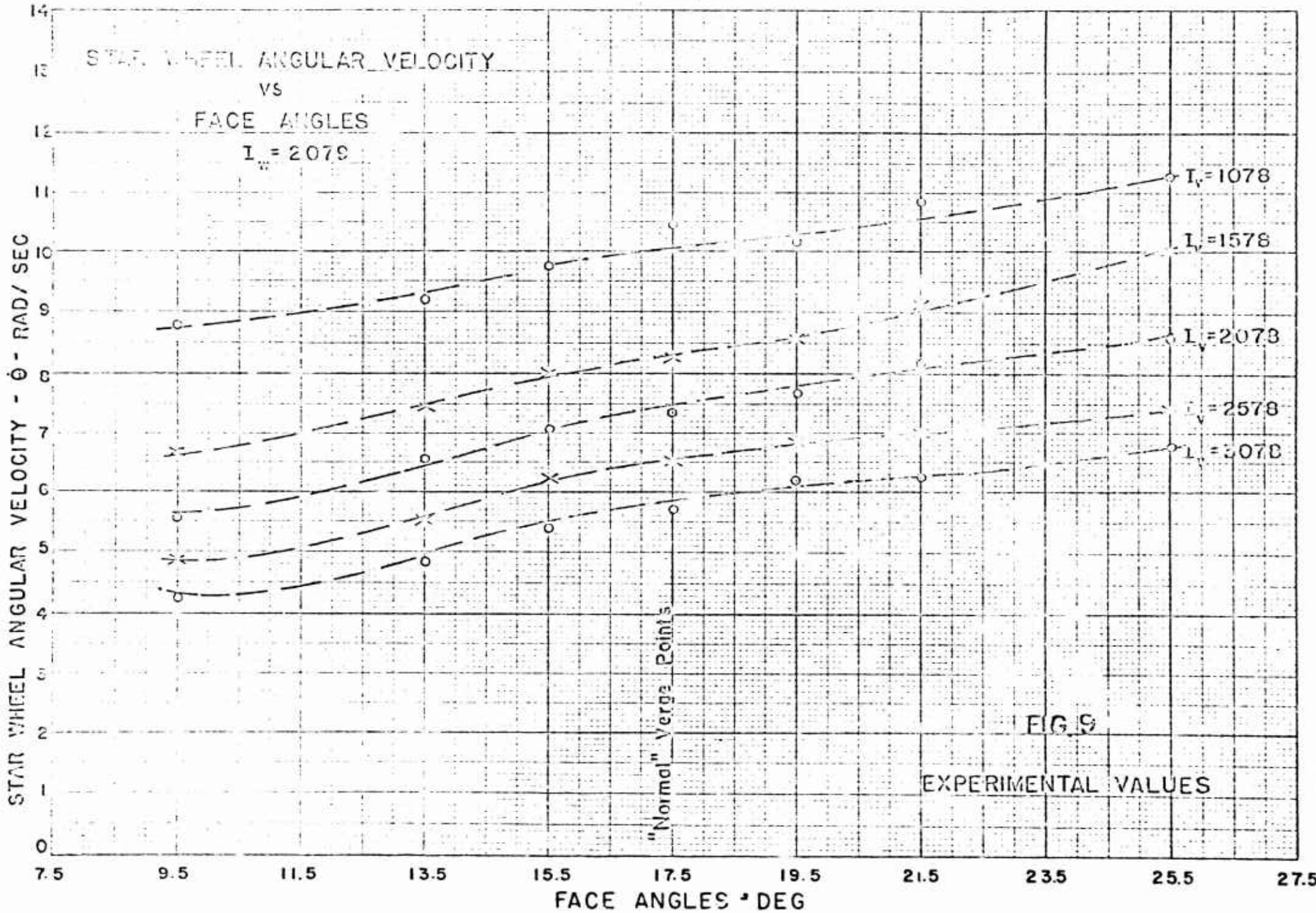

FIG. 9

EXPERIMENTAL VALUES

Finally we have plotted on Fig. 10, the values of A against the values of β_o, both theoretical and experimental. The obvious result is of course that both curves show that A (and so v) is directly proportional to β_o, within rather close limits. Further, the theoretical curve predicts a change in velocity (from that of the normal case) of about 35% at either extreme. The experimental curve predicts about a 25% change at either extreme. It is also clear by comparision of Figs. 8 and 9 that although the experimental velocity is less than the theoretical velocity for every point, as is to be expected, it is also true that the slope of the experimental curves is less than that for the theoretical. This indicates that for large verge angles (a broad point at the corner) the velocity is much lower than predicted. In such cases, the fundamental considerations upon which the equations are based must be less closely approximated. In particular it is to be remembered that we have always assumed the collision to take place on the point of the tooth. When β_o is large, this is less likely to be true. As a result the collisions take place (in time and in angle) before predicted by our equations. This means less free travel and hence a longer period, therefore a smaller velocity. While not the only factor involved this seems to be the most important reason for the lowered experimental velocities.

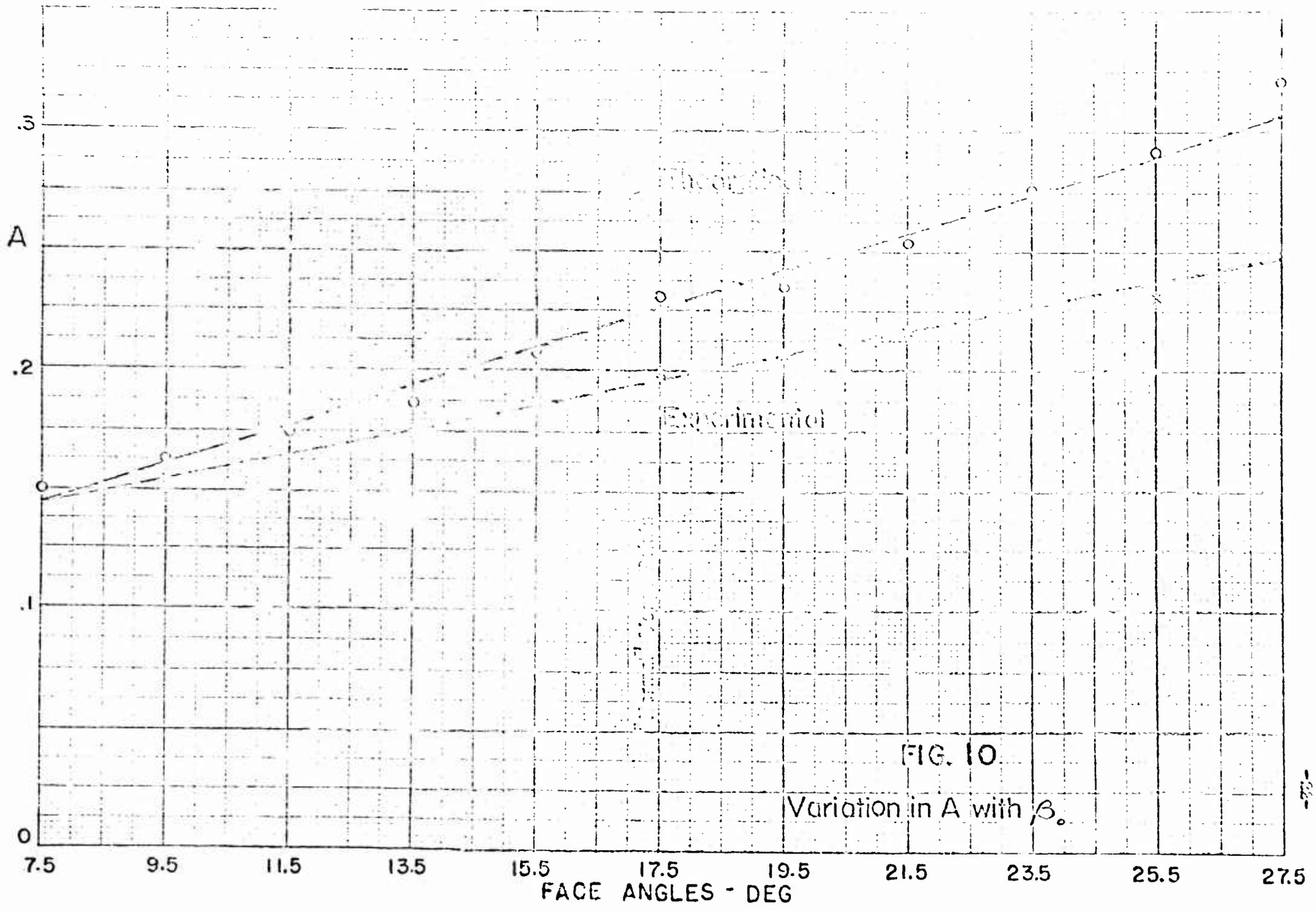

FIG. 10

Variation in A with β_o

VII. EFFECT OF VARIATIONS IN k

In accord with the discussion on limits k was varied over the following values: .2175, .2198, .2210, .2222, .2235, .2245, .2268. For each of these values of k, we computed $\bar{U}$ for I_V = 1033, 2500 and 5000. The results of this computation are given on Fig. 11.

We must note here that the plot of $\bar{U}$ vs k is nearly linear in the case of the light verge, but not for the other two. Proceeding as in the case for variable verge angle, we obtain the following table of constants A.

I_V	.2175	.2198	[illegible]	[illegible]	[illegible]	[illegible]	.2268
1033	.198	.207	[illegible]	[illegible]	[illegible]	[illegible]	.260
2500	.189	.208	.220	.230	.240	[illegible]	.265
5000	-----	.190	.197	.208	.232	[illegible]	.312

The system will not run when I_V = 5000, k = .2175, so there is no value for this case. The results of this calculation do not indicate any correlation between the values of A in each column. It seems most unlikely that the same functional dependence as before can be expected as far as I_V is concerned. Except empirically, there is no usable information here. For the 1033 verge there is a variation of some 15% in velocity above and below that for the normal verge.

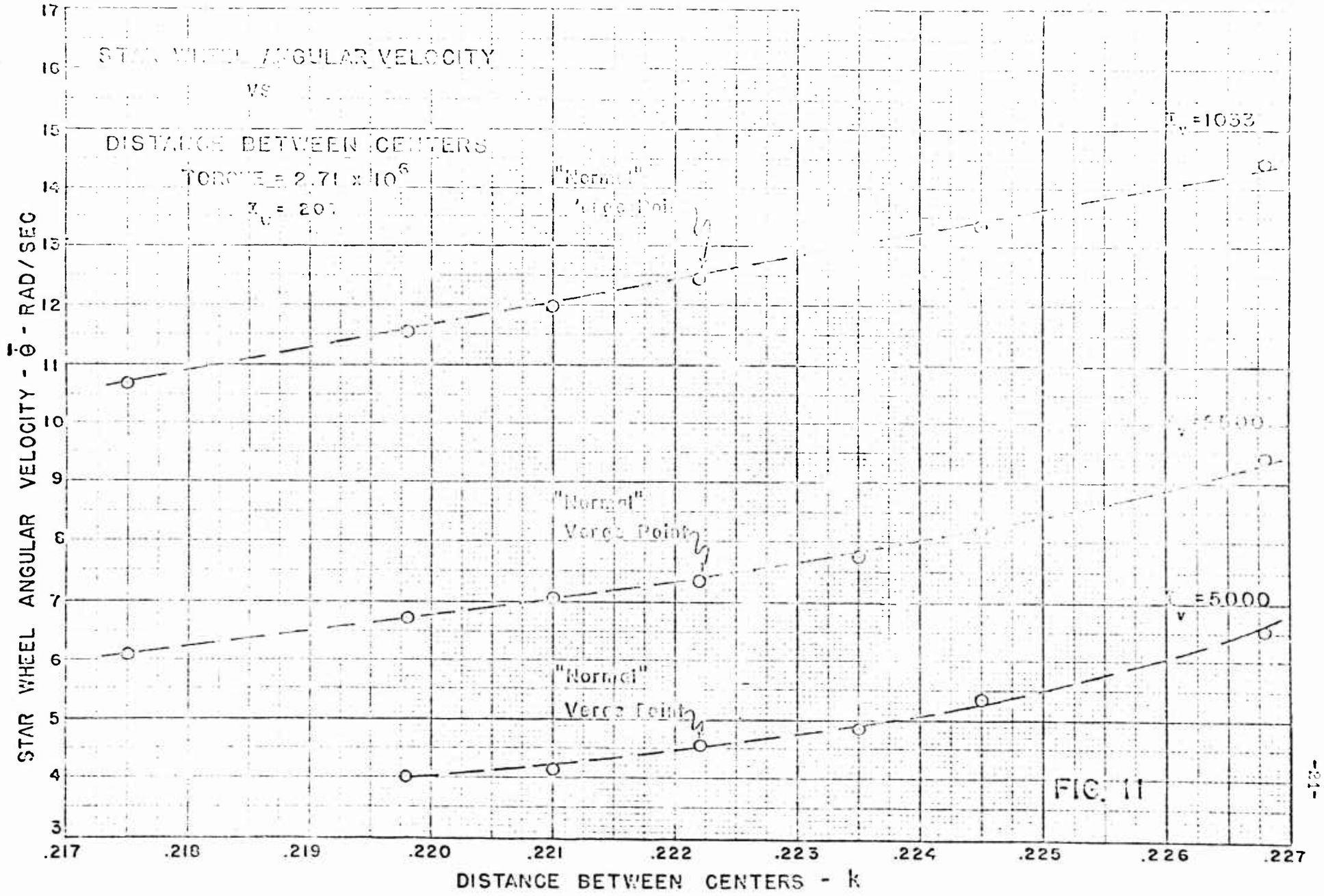
STAR WHEEL ANGULAR VELOCITY
VS
DISTANCE BETWEEN CENTERS
TORQUE = 2.71 x 10^6
"Normal" Verge Point
"Normal" Verge Point
"Normal" Verge Point
STAR WHEEL ANGULAR VELOCITY - θ̇ - RAD/SEC
DISTANCE BETWEEN CENTERS - k
.217
.218
.219
.220
.221
.222
.223
.224
.225
.226
.227
3
4
5
6
7
8
9
10
11
12
13
14
15
16
17

FIG. 11

VIII. EFFECT OF VARIATIONS IN R

As we have shown above, the range of allowable values of R was such that the following values were used: .165, .16775, .1685, .170, .171, .173. For each of these values of R, θ is computed for three values of I_V: 1033, 2500, 5000. The results of these computations are plotted in Fig. 12.

As before we compute the values of constant A in each case, on the basis of the usual functional dependence upon I_V, namely $\theta \sim I_V^{-.612}$. The results are given in the table below.

I_V	.1650	.16775	.1685	.170	.171	.173
1033	.249	.235	.219	.205	.188	.182
2500	.265	.229	.218	.201	.187	----
5000	.296	.218	.200	----	----	----

Once more we conclude that the lack of uniformity in the values of A suggests that as R changes value, the functional dependence of θ on I_V also changes. It is interesting to note here that there is, for each value of I_V, a linear dependence of θ on R, and that each of these lines has about the same slope.

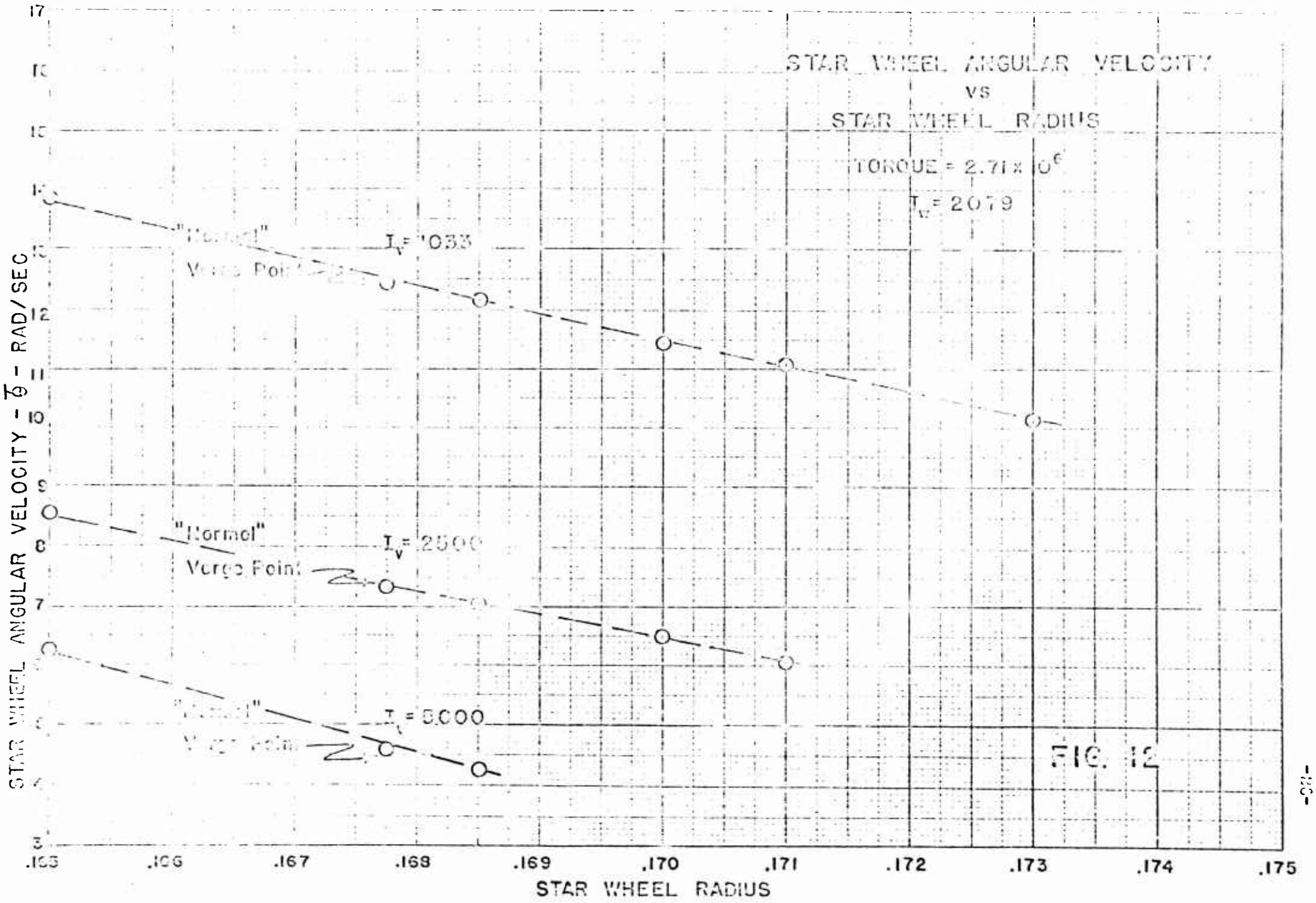
STAR WHEEL ANGULAR VELOCITY
VS
STAR WHEEL RADIUS
TORQUE = 2.71 x 10^6
"Normal" Verge Point
I_V = 1033
"Normal" Verge Point
I_V = 2500
"Normal" Verge Point
I_V = 5000
STAR WHEEL ANGULAR VELOCITY - θ̄ - RAD/SEC
STAR WHEEL RADIUS
17
16
15
14
13
12
11
10
9
8
7
6
5
4
3
.165
.166
.167
.168
.169
.170
.171
.172
.173
.174
.175

FIG. 12

IX. EFFECT OF VARIATIONS IN $(x_o y_o)$

Referring to page 16 of this report we find a list of points $(x_o y_o)$ for which the values of $\bar{\theta}$ were computed, in this case for only two values of I_v, 1033 and 5000. We proceeded as follows: Choosing the smallest allowable value of ρ, we calculated $\bar{\theta}$ for each of three different points such that $\rho^2 = x_o^2 + y_o^2$. This gave us three values and it was noted that as x_o becomes larger (as the points P_1 P_2 P_3 are taken in that order) the values of $\bar{\theta}$ became greater. This holds true for either verge moment, and for all values of ρ chosen.

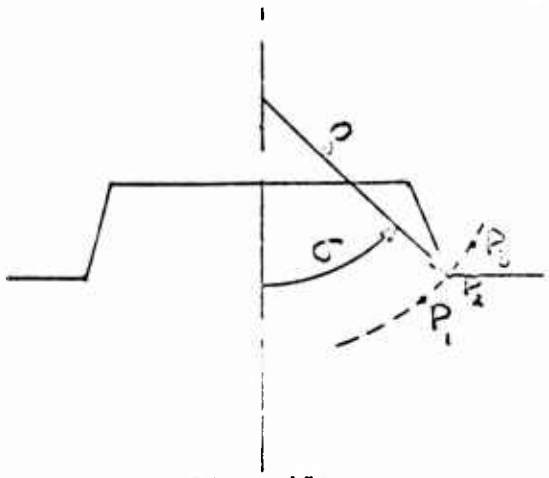

FIG. 13

It was difficult to decide how to plot these results graphically, until it was noted that if values of $\bar{\theta}$ were plotted against a certain angle σ, all points for the 1033 verge lie more or less on a straight line, regardless of ρ or x_o. To a somewhat poorer approximation the same thing is true of the values obtained for the 5000 verge. The angle σ is defined by $\sigma = \sin^{-1} x_o/\rho$, and is shown in Fig. 13. It is the same angle called in IV (D) the angle ψ_o. Approximately, then, the data plotted on Fig. 14 shows that for any given σ, $\bar{\theta}$ is the same regardless of ρ, within the limits over which the points $(x_o y_o)$ may extend.

Reference to Fig. 14 will show this to be true. There are indicated on this graph, three solid black points, which are for $\rho = .1340$ and $x_o = .096$, $.098$, $.100$. Clearly as x_o increases $\bar{\theta}$ increases. One would find a similar situation for points at each of the other values of ρ, and for $I_v = 5000$. Because of the small differences between values of $\bar{\theta}$ for the same σ but different ρ it seems logical to discuss these values on the basis of a linear relationship, $\bar{\theta}$ vs σ as outlined above. We note in passing that actually there appears to be a tendency for $\bar{\theta}$ to be slightly larger as ρ increases for each fixed value of σ, but this is relatively unimportant.

We could here also evaluate the constants A in terms of the function described above, and if this is done it is found once more that as σ changes so does the form of the equation necessary to predict $\bar{\theta}$. Here the "normal" verge point lies at the left end of the curve, and as σ increases to the maximum, there is an increase of some 28% in the velocity for the case $I_v = 1033$, and nearly 50% in the case $I_v = 5000$.

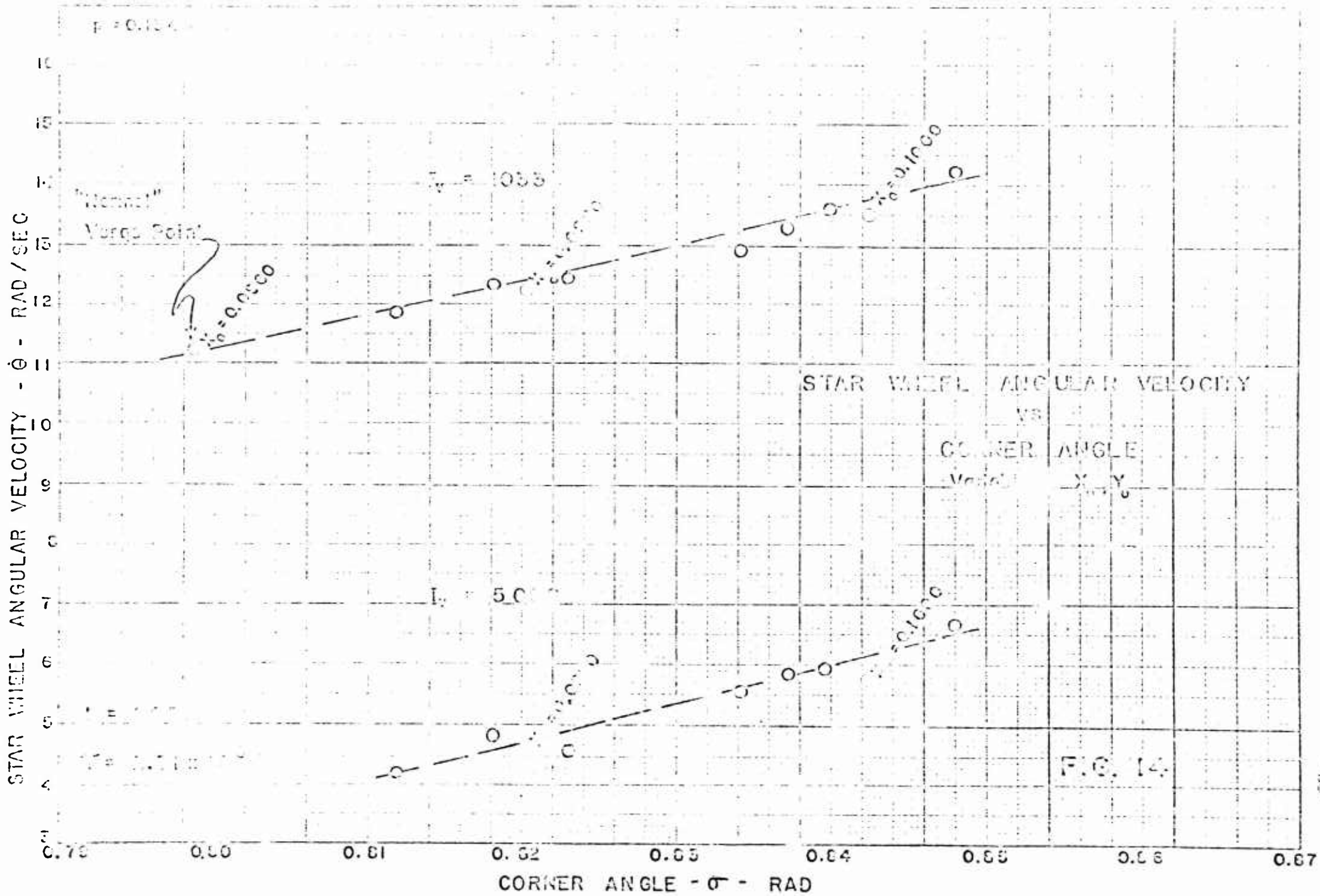
STAR WHEEL ANGULAR VELOCITY
vs
CORNER ANGLE
Variable
X Y
"Normal"
Range Point
STAR WHEEL ANGULAR VELOCITY - Θ̇ - RAD / SEC
CORNER ANGLE - σ - RAD
0.78
0.80
0.81
0.82
0.83
0.84
0.85
0.86
0.87

F.G. 14.

X. ANALYSIS OF RESULTS

From a consideration of the data discussed above, certain facts are clear. Primarily one finds (as is expected) that the empirical equation derived in R holds only for a verge-wheel system of the type called "normal". It is not a generally valid equation for other geometrical shapes. In particular we found that this equation was legitimate when β_o was varied, but not in any other situation. It is difficult to understand why this should be so in the case of the β_o variation. It was first thought that since all values of $\dot{\theta}$ in the cases of variable k, R $(x_o y_o)$ were computed by a different method than used in the case of β_o this might account for the breakdown of the empirical equation. With this in mind, we attempted to fit the values of $\dot{\theta}$ in the case of variable k, R and $(x_o y_o)$ into a single empirical equation of the type used heretofore. This cannot be done, so that it seems logical to conclude that for each different geometry there is a different equation.

A second striking result of our calculations is that in almost all cases the variation of $\dot{\theta}$ as one varies the value of a geometrical factor is fairly well represented by a linear approximation. This is particularly true in the cases of R, and the lighter verges and k. Within the limits set by the problem, our curves will indicate how much change in $\dot{\theta}$ to expect for a given change in R, k or $(x_o y_o)$. One could, if it seemed important, find the linear relationships readily.

It should also be clearly understood that we have never considered changes of more than one geometric factor at a time. The amount of computation necessary to do this seems prohibitive. Certainly, with what we have found, some reasonable predictions could be made. We can say with certainty that any change which tends to increase the time during which the wheel and verge are free of each other tends to speed up the motion. We find this to occur for increasing k, decreasing R or increasing σ. It is not at all obvious that this is occurring in the case of variable β_o however. In this case it appears to be principally a case of a change in the values of u/v. In general, for small β_o, u/v is large and for large β_o u/v is small. This simply means that in a relative sense the torque being applied to slow down the wheel is decreasing as β_o increases so the wheel runs more rapidly. These two factors are, it would seem, the important one governed by geometry. To repeat, these factors are (1) length of time the verge and wheel are free of each other, (2) values of the ratio u/v. In the design of a verge-wheel system this information should be of aid. These conclusions can be compared with the theoretical discussion of Section III.

Of all the geometrical factors studied none can be changed enough to alter the velocity of the "normal" case by more than 50%. Remember again the restriction of "normal" motion. Of these geometric factors, the apparatus might be built so as to make k variable. Then as k is increased from .2172 inches to .2269 inches there will be a continuous and nearly linear change in velocity $\dot{\theta}$. Noting, however, that the total change is less than 10 mils it appears that any accurate method of controlling k would be of costly manufacture. Of course the other dimensions, R, β_o, $(x_o y_o)$ might be changed in the process of manufacture to give verges of different amounts of time delay, but as stated above such changes could not affect the final $\dot{\theta}$, or the final delay time, to a great extent.

It should be remembered, of course, that we have studied only one particular kind of untuned clock mechanism. The possible number of shapes and arrangement is unlimited. It would seem reasonable to expect that for certain types the delay times might depend very strongly on geometric factors. The results reported here might form a basis from which other designs could be worked out.

APPENDIX A SOLUTION FOR THE MOTION OF THE SYSTEM

Reference to Appendix A of R will be helpful in understanding the terms employed in this discussion.

We assume that both wheel and verge are at rest in the position of leading equilibrium at the beginning. Hence in the equation

$$\dot{\theta}_1^2 = \frac{\dot{\theta}_o^2 \left[I_W + I_V \left(\frac{d\alpha}{d\theta} \right)_o^2 \right] + 2\tau(\theta_1 - \theta_o)}{I_W + I_V \left(\frac{d\alpha}{d\theta} \right)_1^2} \qquad (1)$$

$$\dot{\theta}_o = 0, \left(\frac{d\alpha}{d\theta} \right)_o = \frac{u}{v} \text{ at } \theta_o \;, \quad \left(\frac{d\alpha}{d\theta} \right)_1 = \frac{u}{v} \text{ at } \theta_1$$

where θ_1 is the angle of last contact leading. Having computed $\dot{\theta}_1$, then

$$\dot{\alpha}_1 = \left(\frac{d\alpha}{d\theta} \right)_1 \cdot \dot{\theta}_1$$

Having reached and passed the position of last contact leading, the wheel and verge turn freely until collision trailing, the position of which is found from

$$t = \frac{\alpha_2 - \alpha_1}{\dot{\alpha}_1} \qquad \theta_2 = \frac{\tau}{2 I_W} \cdot t^2 + \dot{\theta}_1 \cdot t + (\theta_1 - \theta_k) \qquad (2)$$

and the use of the α vs θ curve for trailing contact.

The velocity of the wheel just before and just after this collision are found from equations

$$\dot{\theta}_2 = \frac{\tau}{I_W} t + \dot{\theta}_1$$

and

$$\dot{\theta}_3 = \frac{I_W \dot{\theta}_2 + \left(\frac{d\alpha}{d\theta} \right)_3 \cdot I_V \cdot \left(\frac{d\alpha}{d\theta} \right)_1 \cdot \dot{\theta}_1}{I_W + I_V \left(\frac{d\alpha}{d\theta} \right)_3^2}$$

Of course $\left(\frac{d\alpha}{d\theta} \right)_3 = \frac{u}{v}$ at first contact (collision trailing). It is to be noted then in work reported in R, $u/v = K$ at collision trailing or $u/v = K'$ at collision leading are both considered positive but that $\left(\frac{d\alpha}{d\theta} \right) > 0$ for contact trailing, $\left(\frac{d\alpha}{d\theta} \right) < 0$ for contact leading. The only point at which this is important is in equations (4) and (5) (which follows later) where the numerator always is given by the difference of two numbers, since the $\left(\frac{d\alpha}{d\theta} \right)$ are of opposite sign.

The wheel and verge now being in trailing contact we have

$$\dot{\theta}_4^2 = \frac{\dot{\theta}_3^2 \left[I_W + - \frac{(d\alpha)^2}{(d\theta)_3} \right] + 2\,T\,(\theta_4 - \theta_3)}{I_W + I_V \frac{\left(\frac{d\alpha}{d\theta}\right)_4^2}{}} \qquad (5)$$

where $\frac{(d\alpha)}{(d\theta)_4} = \frac{u}{v}$ at last contact leading. Also we get

$$\dot{\alpha}_4 = \frac{(d\alpha)}{(d\theta)_4} \cdot \dot{\theta}_4$$

Now if I_V is large enough, it is possible for $\dot{\theta}_3$ to be negative, indicating that the wheel has reversed direction at the collision. Under these circumstances it is necessary to find the angle θ_{3A} at which the wheel come to rest before starting forward again.

This angle is found by using equation (5) where $\theta_{3A} = \theta_4 < \theta_3$ and $\dot{\theta}_{3A}^2 = \dot{\theta}_4^2 = 0$.

Now

$$\theta_{3A} = \theta_3 - \frac{\dot{\theta}_3^2 \left[I_W + I_V \frac{(d\alpha)^2}{(d\theta)_3} \right]}{2\,T} \qquad (6)$$

At θ_{3A} the wheel is at rest. As it once more moves forward it returns to θ_3 at which it now has a velocity $\dot{\theta}_3 > 0$.

The remainder of the cycle up to leading collision is carried out as described above, using equations

$$t = \frac{\alpha_5 - \alpha_4}{\dot{\alpha}_4} \qquad \theta_5 = \frac{T}{2\,I_W} \cdot t^2 + \dot{\theta}_4 \cdot t + (\theta_4 + \theta_k) \qquad (7)$$

then

$$\dot{\theta}_5 = \frac{T}{I_W} \cdot t + \dot{\theta}_4$$

and

$$\dot{\theta}_6 = \frac{I_W \dot{\theta}_5 + \frac{(d\alpha)}{(d\theta)_6} \cdot I_V \cdot \frac{(d\alpha)}{(d\theta)_4} \cdot \dot{\theta}_4}{I_W + I_V \frac{\left(\frac{d\alpha}{d\theta}\right)^2}{(d\theta)_6}} \qquad (9)$$

where $\dot{\theta}_6$ is the velocity of the wheel immediately after leading collision.

If $\dot{\theta}_0 < 0$ we use equation (1) to find [illegible] the angle to which the wheel backs up and comes to rest before beginning its forward motion once more.

$$\theta_{\theta_A} = \theta_0 - \frac{\dot{\theta}_0^2 \left[I_w + I_y \left(\frac{\quad}{\quad} \right)^2 \right]}{2 \, T} \qquad (10)$$

As the wheel moves forward to θ_0 it has now the velocity $\dot{\theta}_0 > 0$.

One cycle has been completed. The values θ_0 and $\dot{\theta}_0$ found above are now considered as the θ_0 and $\dot{\theta}_0$ for a second cycle. The computation is repeated. After three or perhaps four such sets of computations it is found that equilibrium has been reached, in the sense that each velocity of the last cycle is equal to the corresponding velocity of the preceding cycle.

In order to plot $\dot{\theta}$ vs θ, it is usually necessary to compute certain intermediate values of θ. These calculations are carried out as described in R, Appendix A, using the equations of the present discussion of course. Once the curve $\dot{\theta}$ vs θ has been obtained we proceed as described in R.

APPENDIX B VERGE DESIGN FOR CONSTANT u/v

In Section II of this report an assumption was made that there existed a verge in which the ratio of lever arms u/v would remain constant as the verge moved. The accompanying figure shows where these lever arms are measured. The equation is

$$\frac{u}{v} = -\frac{R\cos(\beta+\theta)}{k\cos\beta + R\cos(\beta+\theta)}$$

where $k < 0$, as usual. Now as the tooth moves along the face, the perpendicular which determines u/v (which is P P') is rotated, hence the ratio u/v will in general change. For the plane pallet faces used on all verges studied in this work the angle θ measures simply the angular position. Another way of saying this is that as the wheel rotates the line P P' changes direction only because the verge is rotating.

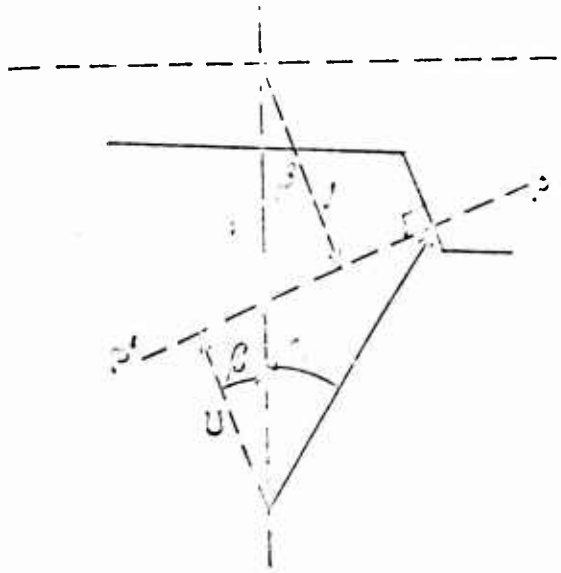

FIG. 15

Now if the pallet face is not plane but a curved surface of some type, the direction of P P' changes as the wheel rotates for two reasons, first because the verge itself is rotating and second because the direction of P P' at the new point of contact is not the same as at the original point because of the curvature of the surface.

Suppose we equate the expression for u/v to a constant and compute the β corresponding to each θ. This value of β now can refer only to the angle of lever arm u with axis of centers, and not specifically to the rotation of the verge. Suppose these values of β just computed be compared with values computed in a similar case for the plane face verge. The difference in each pair of values should be a measure (approximate) of the angle the tangent to the curved surface makes with the plane surface at that value of θ. Using a graphical method one may sketch the curved surface. This surface is in error because we have carried out our calculations on the basis that the tooth is in contact with the plane face at each angle. In reality, the tooth must be in contact with the curved pallet face. In order to see how to apply a correction for this we consider a specific case.

The "normal" verge at l[illegible] equilibrium gives a lever arm ratio u/v = .949. We computed, [illegible] range of values of θ either side of the equilibrium point, those [illegible]ues of β required to keep u/v constant. Then using the values of β originally computed for the rotation of the plane faced verge, we found the increments $\Delta\beta$ at each θ by which a normal to the verge surface must change. The full line plotted in the following diagram, Fig. 16, is the result of this approximate solution. As the curve departs further from the line it turns out that our values of $\Delta\beta$ become too large. In other words the curve is somewhat flatter than that drawn as a solid line. The dotted line is probably more nearly correct.

This dotted line curve was not comput[illegible]. One could proceed as follows, however. From the graphical plot of the accom[illegible]ying figure it is possible to determine how much the verge would be rotated when the tooth is in contact at point A' rather than A. This $\Delta\beta'$ could then be subtracted from the increment $\Delta\beta$ above to give a more nearly correct slope angle at that point.

An approach of this type should make it fairly simple to design a pallet face which would produce constant u/v. It is of course obvious that the preceding discussion is only semi-quantitative at best.

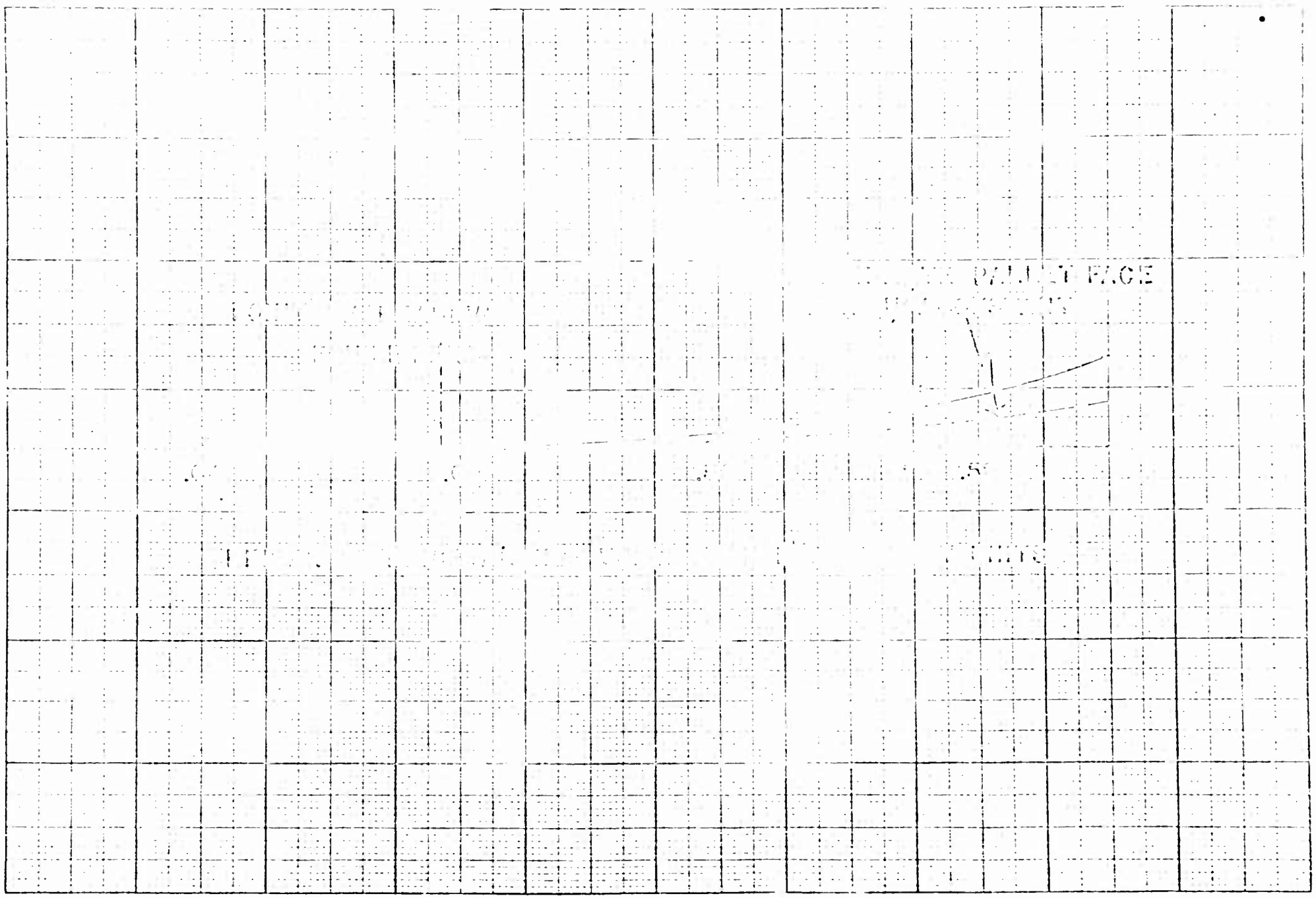

FIG. 16

FIGURE 4
SHOWING THE TORN DOWN
INITIATOR NO. 541

FIGURE 5
SHOWING THE TORN DOWN
INITIATOR NO. 542

FIGURE 6
SHOWING THE TORN DOWN
INITIATOR NO. 547